

Nutrient resupplementation arrests bio-oil accumulation in *Phaeodactylum tricornutum*

J. Valenzuela · R. P. Carlson · R. Gerlach · K. Cooksey ·
B. M. Peyton · B. Bothner · M. W. Fields

Received: 18 March 2013 / Revised: 16 May 2013 / Accepted: 19 May 2013 / Published online: 15 June 2013
© The Author(s) 2013. This article is published with open access at Springerlink.com

Abstract *Phaeodactylum tricornutum* is a marine diatom in the class Bacillariophyceae and is important ecologically and industrially with regards to ocean primary production and lipid accumulation for biofuel production, respectively. Triacylglyceride (TAG) accumulation has been reported in *P. tricornutum* under different nutrient stresses, and our results show that lipid accumulation can occur with nitrate or phosphate depletion. However, greater lipid accumulation was observed when both nutrients were depleted as observed using a

Electronic supplementary material The online version of this article (doi:10.1007/s00253-013-5010-y) contains supplementary material, which is available to authorized users.

J. Valenzuela · B. Bothner
Department of Chemistry and Biochemistry,
Montana State University, Bozeman, MT, USA

J. Valenzuela · R. P. Carlson · R. Gerlach · B. M. Peyton ·
M. W. Fields
Center for Biofilm Engineering, Montana State University,
Bozeman, MT, USA

R. P. Carlson · R. Gerlach · B. M. Peyton
Department of Chemical and Biological Engineering,
Montana State University, Bozeman, MT, USA

K. Cooksey · M. W. Fields
Department of Microbiology, Montana State University,
Bozeman, MT, USA

M. W. Fields
National Center for Genome Resources, Santa Fe, NM, USA

R. P. Carlson · R. Gerlach · B. M. Peyton · B. Bothner ·
M. W. Fields
Thermal Biology Institute, Montana State University,
Bozeman, MT, USA

M. W. Fields (✉)
Department of Microbiology, Center for Biofilm Engineering,
Montana State University, 366 EPS Building,
Bozeman, MT 59717, USA
e-mail: matthew.fields@erc.montana.edu

Nile Red assay and fatty acid methyl ester (FAME) profiles. Nitrate depletion had a greater effect on lipid accumulation than phosphate depletion. Lipid accumulation in *P. tricornutum* was arrested upon resupplementation with the depleted nutrient. Cells depleted of nitrogen showed a distinct shift from a lipid accumulation mode to cellular growth post-resupplementation with nitrate, as observed through increased cell numbers and consumption of accumulated lipid. Phosphate depletion caused lipid accumulation that was arrested upon phosphate resupplementation. The cessation of lipid accumulation was followed by lipid consumption without an increase in cell numbers. Cells depleted in both nitrate and phosphate displayed cell growth upon the addition of both nitrate and phosphate and had the largest observed lipid consumption upon resupplementation. These results indicate that phosphate resupplementation can shut down lipid accumulation but does not cause cells to shift into cellular growth, unlike nitrate resupplementation. These data suggest that nutrient resupplementation will arrest lipid accumulation and that switching between cellular growth and lipid accumulation can be regulated upon the availability of nitrogen and phosphorus.

Keywords Algae · Diatom · Lipid · Biofuel · Nitrate · Phosphate

Introduction

In modern societies, petroleum-based products and fuels have strongly influenced human society and infrastructure. In the case of fossil fuels, supply and demand over the past hundred years has been relatively equal; however, increased contemporary consumption has had undesirable consequences (Brown, L.R. 2006). Petroleum markets have become increasingly unpredictable causing destabilized fuel prices. Additionally, the environmental impacts of the release of the greenhouse gas carbon dioxide (CO₂) from the

combustion of fossil fuels without balanced CO₂ sequestration has likely contributed to increases in atmospheric CO₂ levels. For example, the amount of carbon released (44×10^8 g) in 1 year from the consumption of fossil fuels is 400-fold more than the amount of carbon that can be fixed via net global primary productivity (Dukes 2003). In order to offset the massive influx of CO₂ into the atmosphere, the utilization of renewable biofuels (e.g., ethanol, butanol, H₂, CH₄, and biodiesel) is needed. Moreover, the use of autotrophic microorganisms for the production of biomass, biochemicals, and biofuels can further contribute through the direct utilization of atmospheric CO₂.

Diatoms are unicellular eukaryotic microalgae that account for approximately 40 % of the total marine primary production each year (Falkowski and Raven 1997; Field 1998; Granum et al. 2005). Diatoms and green microalgae are photoautotrophs that use CO₂ as a carbon source and sunlight as an energy source, and many microalgae can store carbon and energy in the form of neutral lipids (e.g., triacylglycerides (TAGs)). Thus, the ability to fix and store carbon as long-chained reduced hydrocarbons that can be converted into biodiesel makes algal lipids a potential renewable and carbon neutral energy source. Chisti (2007) estimated conservatively (25–30 % as lipid content, w/w) that it would only take 3 % of the arable cropland in the US growing microalgae for biodiesel to replace 50 % of transportation fuel needs in the US (Chisti 2007). Although the interest in algal biofuels has been reinvigorated (Courchesne et al. 2009; Greenwell et al. 2010), significant fundamental and applied research is still needed to fully maximize algal biomass and biochemical production for biofuels. In addition to CO₂ utilization, algal biomass production can also be coupled to wastewater resources (e.g., water, N, and P), and wastewater from agricultural, industrial, and municipal activity may provide a cost-effective source of nutrients needed for algal growth. Agricultural and municipal wastewater can be high in nitrogen (N) and phosphorus (P) (Aslan and Kapdan 2006; Hoffmann 2002; Mallick 2002; Pittman et al. 2011), and thus, there is great potential for the integration of wastewater treatment and algal biofuel production. However, an improved understanding of the relationship between the effects of N and P availability on cellular resource allocation (cell growth versus lipid storage) in microalgae is needed.

Phaeodactylum tricorutum is a marine diatom in the class Bacillariophyceae, and the Bacillariophyceae are one of the most diverse groups of photoautotrophic eukaryotes with >100,000 extant species (Hildebrand 2008; Round et al. 1990). *P. tricorutum* has been extensively studied since being isolated in 1956 and has been characterized into 10 different strains based upon genetic and phenotypic attributes (Martino et al. 2007). The genome sequence of *P. tricorutum* 8.6 (CCAP 1055/1; CCMP2561; morphological strain Pt1) was

determined at 27.4 Mb with over 10,000 gene predictions (Bowler et al. 2008). The chloroplast genome was also sequenced and 162 genes from 117,000 bp were predicted (Oudot-Le Secq et al. 2007). This extensive research background and availability of genomic data makes *P. tricorutum* an ideal model organism for understanding fundamentals of cellular processes and regulation (e.g., lipid accumulation) in diatoms.

TAG accumulation has been well documented as a result of nutrient stress or nutrient deficiency in microalgae (Gardner et al. 2010; Sheehan 1998), and in particular, nitrate and/or phosphate stress can cause lipid accumulation in numerous algae (Hu et al. 2008). Recently, we observed that phosphorus limitation can initiate lipid accumulation and is magnified by nitrogen limitation in *P. tricorutum* Pt1 (Valenzuela et al. 2012). In this study, we examined (1) the effects of nitrogen and phosphorus depletion on lipid accumulation and (2) the temporal effects of nutrient resupplementation on biomass growth and lipid accumulation. Our results show that N and P levels contribute to cell switching from a cellular growth state to a lipid accumulation state and that lipid accumulation can be arrested and potentially reversed dependent upon nutrient availability.

Materials and methods

Culture and growth conditions

The Bohlin Strain 8.6 of *P. tricorutum* (Pt1, CCMP2561 [Culture Collection of Marine Phytoplankton, now known as NCMA: National Center for Marine Algae and Microbiota], genome sequenced) was used in all experiments. The diatom Pt1 was grown in ASPII medium (Tris base buffered; pH of 8.2) as previously described (Cooksey and Cooksey 1974; Provasoli et al. 1957; Valenzuela et al. 2012). Cells were grown in temperature-controlled photobioreactors (1.25 L) at 20 °C. Light was provided at $450 \mu\text{E}^{-1} \text{s}^{-1} \text{m}^2$ on a 14:10 light:dark cycle. Each reactor tube was aerated with sterile ambient air at a rate of 0.40L min^{-1} with the CO₂ from air as the sole source of carbon. Cells for inocula were grown photoautotrophically for two generations and then transferred to the 1.25-l photobioreactors when cells were in exponential phase to achieve a final concentration of approximately 1×10^5 cells ml⁻¹. The only sources of nitrogen (N) and phosphorus (P) were nitrate (NaNO₃) and phosphate (H₂KPO₄), respectively. To test replete conditions of N, P, or both N+P, cells in photobioreactors were resupplemented daily with approximately 1.5 ml of filter-sterilized 300 mM NaNO₃ or 28.7 mM H₂KPO₄. Contamination was checked throughout the experiments by plating on R2A agar and ASPII medium supplemented with 0.5 % glucose and yeast extract.

Experimental design

The response of lipid accumulation in *P. tricornutum* (Pt1) to nutrient stress was tested in a temporal fashion under nutrient-deplete and nutrient-replete conditions. For replete conditions, N, P, or both N+P were kept in excess throughout batch growth. If N was replete, then the limiting nutrient was P, and vice versa, in P-replete conditions, N became limited. For N+P-replete conditions, both N and P were maintained in excess with sequential daily additions during growth (Table 1). To test whether initial lipid accumulation was reversible, resupplementation experiments were conducted. Cells were allowed to enter stationary phase, where lipid accumulation was observed under N+P depletion and then cells were resupplemented (189 h) with N, P, or both N+P. Therefore, if resupplemented with N, then cells remained P deplete and if resupplemented with P the cells remained N deplete. In addition, N+P was supplied to elucidate the effect of complete nutrient resupplementation postlipid accumulation. Control conditions for both nutrient-replete and resupplementation conditions only contained nutrients from the original medium and, thus, became depleted of N and P and accumulated lipids. Each condition was performed with biological duplicates and compared to standard ASPII controls.

Physiological parameter analysis

During growth, samples were collected and analyzed daily for cell number, chlorophyll *a*, pH, dissolved inorganic carbon (DIC), nitrate, phosphate, and relative neutral lipid abundance via Nile Red (NR) fluorescence. Periodically, cells were collected for fatty acid methyl ester (FAME) analysis using gas chromatography–mass spectrometry (GC–MS). Cell density was monitored via direct cell counts in duplicate with a hemocytometer. Cells were collected (1 ml in triplicate) and centrifuged (10,625×g, 10 min, 4 °C). The supernatant fraction was used for exogenous nitrate and phosphate determinations. To extract chlorophyll, 100 % methanol (1 ml) was added to the cell pellet, vortexed (30 s), and incubated for 24 h

Table 1 Description of tested conditions. Both nitrate and phosphate are depleted during growth in the control. The P-depleted culture has depleted phosphate but nitrate is resupplemented. The N-depleted culture has depleted nitrate but phosphate is resupplemented. The N & P replete culture has both nitrate and phosphate added back to the medium

Condition	Nitrate	Phosphate
Control	↓	↓
P depleted	↑	↓
N depleted	↓	↑
N & P replete	↑	↑

at 4 °C in the dark. The cellular debris was then pelleted (10,625×g, 5 min) and extracts were measured on a spectrophotometer (UV-1700 PharmaSpec UV–vis, Shimadzu). Absorbance was read at 652 and 665 nm to measure chlorophyll *a* and calculated in micrograms per milliliter (Porra 2002). The medium pH was monitored using a standard lab bench pH meter. Cell culture (7 ml) was filtered through a 0.2-µm nylon membrane filter in preparation for DIC availability measurement on a Formacs^{HT} TOC/TN Analyzer (Skalar, Buford, GA, USA). Colorimetric assays were used according to manufacturer protocols to measure nitrate (Szechrome NAS, Polysciences, Inc.) and phosphate (Sensolyte MG Phosphate Assay Kit, AnaSpec). N and P assay absorbance was measured on a black-walled clear-bottom 96-well plate using a Synergy H1 Hybrid Reader (BioTek) spectrophotometer. For cellular lipid levels, the Nile Red assay protocol was used as previously described (Cooksey et al. 1987). Cell culture (1 ml) was diluted to an amount that fit within a linear relationship of Nile Red signal to cell abundance and stained with Nile Red as previously described (Valenzuela et al. 2012).

Microscopy

Fluorescent images were taken with a Nikon Eclipse E800 epifluorescence microscope. Nile Red stained cells were imaged with a B2A (Ex 470/40, DM 500LP, EM515) filter with a 60×/1.20NA WI objective. Color images were captured using an Infinity 2 color camera and Infinity Capture software.

Fatty acid extraction and identification via GC–MS

At different time points of growth, cell culture (10 ml in triplicate) was filtered with Whatman polycarbonate filters (22 mm, 0.2 µm), transferred to microcentrifuge tubes, and immediately flash frozen in liquid nitrogen. To extract lipids, cells were washed off filters with 10 mM Tris–HCl in glass culture tubes and lysed using sonication (1 min) in 2:1 dichloromethane:methanol (1 ml). Cell debris and phase separation was achieved via centrifugation (2 min at 2,750×g). The aqueous layer was removed and the organic layer was transferred to a clean GC vial. Additional 2:1 dichloromethane:methanol (0.5 ml) was added to the cell debris, resonicated, and the organic layer added to the previous organic extract. An internal standard (pentadecanoic acid, C₁₅H₃₀O₂, Sigma-Aldrich) was added to monitor the degree of transesterification. The organic layer was dried under a stream of N₂ at 60 °C. To the dried organic layer, borontrifluoride–methanol (10 % w/w, 400 µl; Sigma-Aldrich) was added for fatty acid transesterification. Vials were incubated at 60 °C for 30 min and then the reaction was quenched with nanopure water (200 µl). The sample

volatile material was dried under N_2 and hexane (0.5 ml) was added to separate FAMES into the organic layer. Saturated NaCl was added to aid in separation of hydrophilic and hydrophobic phases. The hexane layer was then transferred into a new GC vial and dried under N_2 and resuspended in hexane (100 μ l)-concentrating FAMES. The contents were transferred into clean 150- μ l glass inserts within new GC vials. Identification and quantification were done on an Agilent Technologies 5975C inert EI/CI MSD with Triple Axis Detector with a Phenomex ZB-FFAP 250 °C 60 m \times 250 μ m \times 0.25- μ m column and Agilent 7693 autosampler. Carrier gas (He) was set at a flow rate of 2 ml/min at 41.56 psi. Temperature program consisted of ramping phases: 120 to 170 °C for 11.7 min (rate of 6.5 °C/min) followed by a second ramping from 170 to 250 °C for 29.09 min (rate of 2.75 °C/min) and a 9-min holding time at 250 °C. Standard curves were used to quantify FAMES based on integrated chromatogram peak area using Agilent MassHunter Qualitative Analysis software. A standard curve was made with pentadecanoic acid at different molar concentrations and used on individual GC runs. Each peak was quantified based on chromatogram peak area, and a linear best-fit equation was applied to correlate peak area and molar concentration. FAMES were identified by comparison to the spectral data in the National Institute of Standards and Technology Mass Spectral Library (NIST 08) and only the “original” fatty acids were plotted. Only peaks identified with a minimal match score of 50 or greater were considered and were then cross-referenced with the NIST MS Search 2.0 program for confirmation of FAMES species.

Results

Control (N and P depleted)

In *P. tricornutum* (Pt1), nutrient stress has been shown to cause lipid accumulation (Mus et al. 2013; Valenzuela et al. 2012). In control cultures inoculated with approximately 10^5 cells/ml in ASPII medium, exogenous phosphate was depleted within approximately 72 h, while nitrate was depleted within approximately 100 h (Fig. 1b). The medium pH started at 8.2, increased to 8.5 during growth, and decreased back to 8.2 during stationary phase. Cells did not reach stationary phase until two doublings after phosphate was depleted and one doubling after nitrogen was depleted (119 h) (Fig. 1a). Growth after the depletion of exogenous phosphate is most likely a result of intracellular phosphate storage, and Pt1 has been shown to store intracellular phosphate (Leitao et al. 1995). The doubling of cells after nitrogen depletion can be attributed to the repurposing of nitrogen-rich molecules (e.g., chlorophyll) (Fig. 1c).

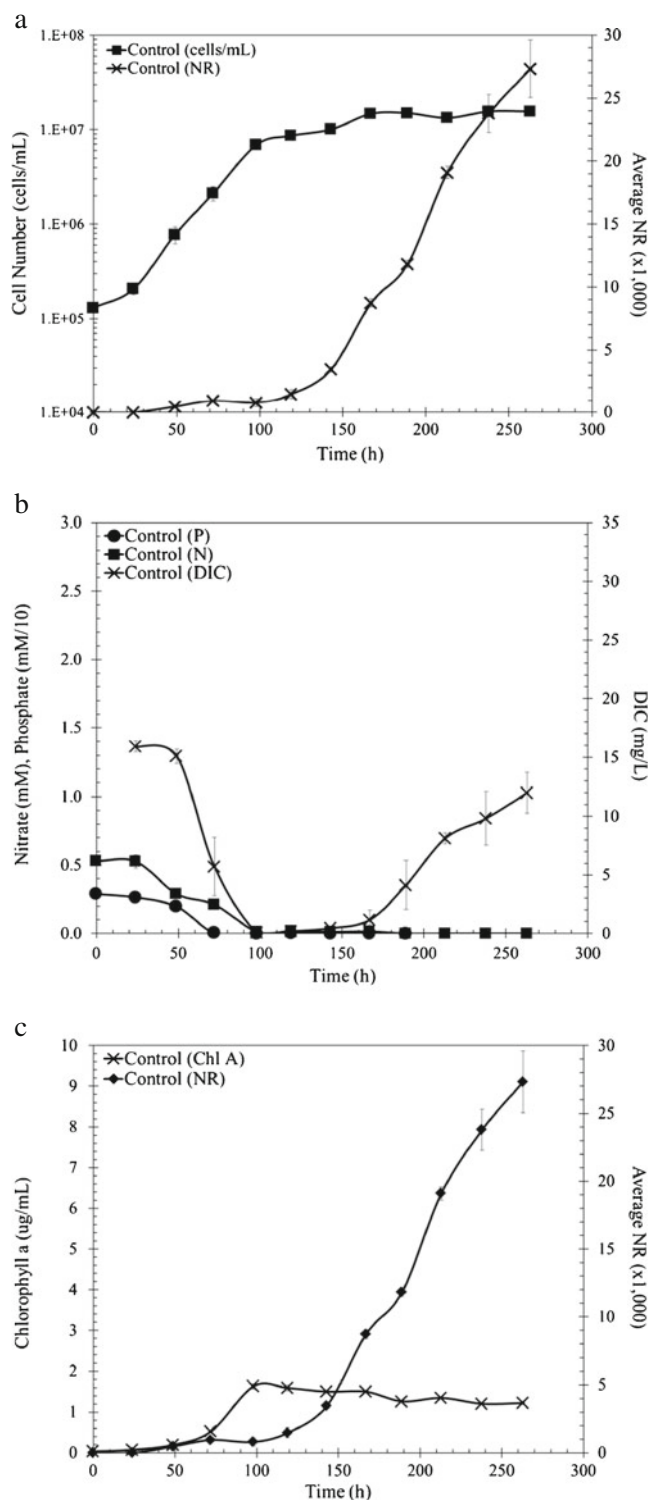


Fig. 1 *P. tricornutum* growth parameters under control conditions, no nutrient resupplementation. **a** Growth curve cells per milliliters (filled square) and Nile Red fluorescence intensity (cross). **b** DIC (cross), NO_3^- (filled square), PO_4^{3-} (filled circle) throughout growth, (phosphate was multiplied by a scaling factor of 10). **c** Chlorophyll a (cross) concentrations and Nile Red fluorescence intensity (filled diamond)

Chlorophyll *a* reached a maximum level at approximately 100 h and the levels declined throughout the rest of the growth curve. The decrease in chlorophyll content correlates to the decrease in nitrate availability, and these results suggest a shift to slower growth and eventual cell cycle cessation. Cells could also be recycling nitrogen from nonessential proteins, which could be a much greater nitrogen source than chlorophyll (Lee et al. 2012; Mus et al. 2013). These data suggest cells reallocated nitrogen resources to maintain functionality during a metabolism shift to lipid accumulation during N depletion.

Nile Red (NR) fluorescence intensity is an indicator of neutral lipid content and there was a slight increase in fluorescence after phosphate was depleted. However, a more drastic increase in NR signal was observed once nitrate was depleted and cells entered stationary phase (Fig. 1a). The specific fluorescence is the NR signal divided by cell numbers. When cells exited exponential phase (119 h), the specific fluorescence was 1.7 and increased 10.3-fold to 17.5 (263 h) as cells remained in stationary phase (Fig. S1b). Cells did not have access to nitrogen or phosphorus but were still able to fix carbon as it was continually being sparged into the system and reducing equivalents were presumably available from photosynthesis. In the exponential phase, the DIC became “limited,” but not depleted (Fig. 1b). However, the DIC recovered as cells entered stationary phase during lipid accumulation. The fixed carbon is presumably going into lipid as cell number, protein, and carbohydrate content do not increase (Valenzuela et al. 2012). These results suggested that the DIC requirement for lipid accumulation is lower than the DIC requirement during cellular exponential growth.

P depletion (N-replete and resupplementation effects)

To distinguish the effects of phosphate alone on lipid accumulation, we maintained nitrogen-replete conditions as phosphate was depleted. There was no difference in the growth rates between control and nitrogen-replete cells or the nitrogen-resupplemented cells. In nitrate-replete conditions, phosphate was depleted at 92 h and a slight increase in NR fluorescence was observed (approximately twofold, Fig. 2a). As nitrate remained in excess during N-replete conditions, the DIC was limited as the carbon requirement for cellular growth was high and resulted in low lipid yields (Fig. 2b). To test nitrogen resupplementation, nitrate was resupplied (189 h) after initial nitrate depletion and an increase in cell number was observed (Fig. 2a). Congruently, a decrease in lipid accumulation was observed postnitrate amendment (sevenfold decrease in NR fluorescence between 189 and 263 h) (Fig. 2a). As with nitrate-replete conditions, DIC concentrations rebounded, as there was no high carbon requirement for growth but a smaller requirement for lipid accumulation prior to resupplementation. However, when resupplemented with

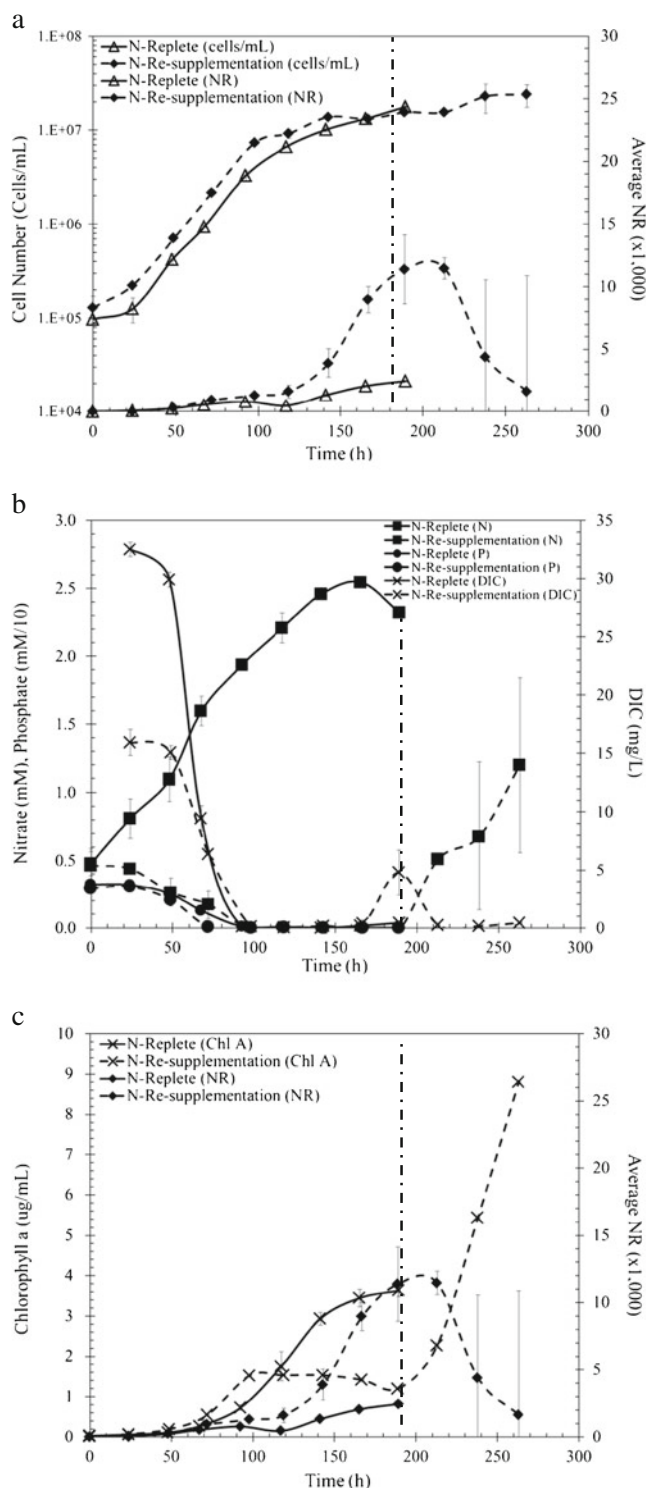


Fig. 2 *P. tricornutum* growth parameters during continued N replete conditions (solid lines) and N resupplemented (dashed lines), meaning phosphorus stress conditions. The dashed vertical line indicates where N was resupplemented at 189 h. **a** Growth curve cells per milliliter (unfilled triangle, filled diamond) and Nile Red fluorescence intensity (filled triangle, filled diamond). **b** DIC (cross), NO_3^- (filled square), PO_4^{3-} (filled circle) throughout growth (phosphate was multiplied by a scaling factor of 10). **c** Chlorophyll *a* (cross) concentrations and Nile Red fluorescence intensity (filled diamond)

nitrate, the cells shifted metabolism to cellular growth (increased cell numbers) and the DIC usage increased (i.e., DIC concentrations decreased) as lipid levels declined. Chlorophyll *a* increased with nitrogen-replete conditions as expected and, when nitrate was resupplemented after stationary phase, an increase in chlorophyll *a* (Fig. 2c) was observed, and these results suggest a switch from lipid accumulation to biomass production during nitrate assimilation.

N depletion (P-replete and resupplementation effects)

Growth rates during phosphate-replete and phosphate-resupplemented conditions were similar to controls (Fig. 3a). Cell numbers did not increase when resupplemented with phosphate as was observed when nitrogen was resupplemented. During replete conditions, phosphate remained elevated and nitrate was depleted at 92 h (Fig 3b). After depletion of nitrogen, the lipid content increased 4.4-fold in specific NR fluorescence units (Fig. 3a, Fig. S1a). After phosphate resupplementation (189 h), lipid content declined, but not to the extent observed during nitrogen resupplementation. Additionally, the DIC available during resupplementation conditions rebounded to levels similar to control conditions (Fig. 3b). Chlorophyll *a* was not affected by excess phosphate during replete conditions nor did levels change when the growth medium was resupplemented with phosphate (Fig. 3c). These results suggest phosphate resupplementation does not arrest lipid accumulation to the same extent as nitrate resupplementation and shift cells back to a cellular growth mode.

N+P replete and supplementation effects

When cells were provided with excess nitrate and phosphate, the growth rate did not increase. However, when N and P were resupplemented after reaching stationary phase at 189 h, cell numbers and chlorophyll increased (Fig. 4a and c). During replete conditions, N and P remained in excess and DIC remained limited during cellular growth and these results are complementary to the observed low specific NR fluorescence (Fig. 4a, b, Fig. S1a). Cells remained in a cell growth state, as suggested by high chlorophyll content (Fig. 4c). When cells reached stationary phase due to N and P depletion and initiated lipid accumulation, the resupplementation of N and P caused a drastic decrease in lipid content. At 189 h, the NR fluorescence intensity was at 9,070 but declined to a fluorescence intensity of 1,067 within 74 h (Fig. 4a). The 8.5-fold decrease in fluorescence indicated a shift to cellular growth associated with the arrest and consumption of lipids. The DIC levels decreased and remained low post-resupplementation with N and P, and these results indicate that the carbon requirement during cellular growth is higher than for lipid accumulation, as would be predicted from a carbon mass balance (Fig. 4b).

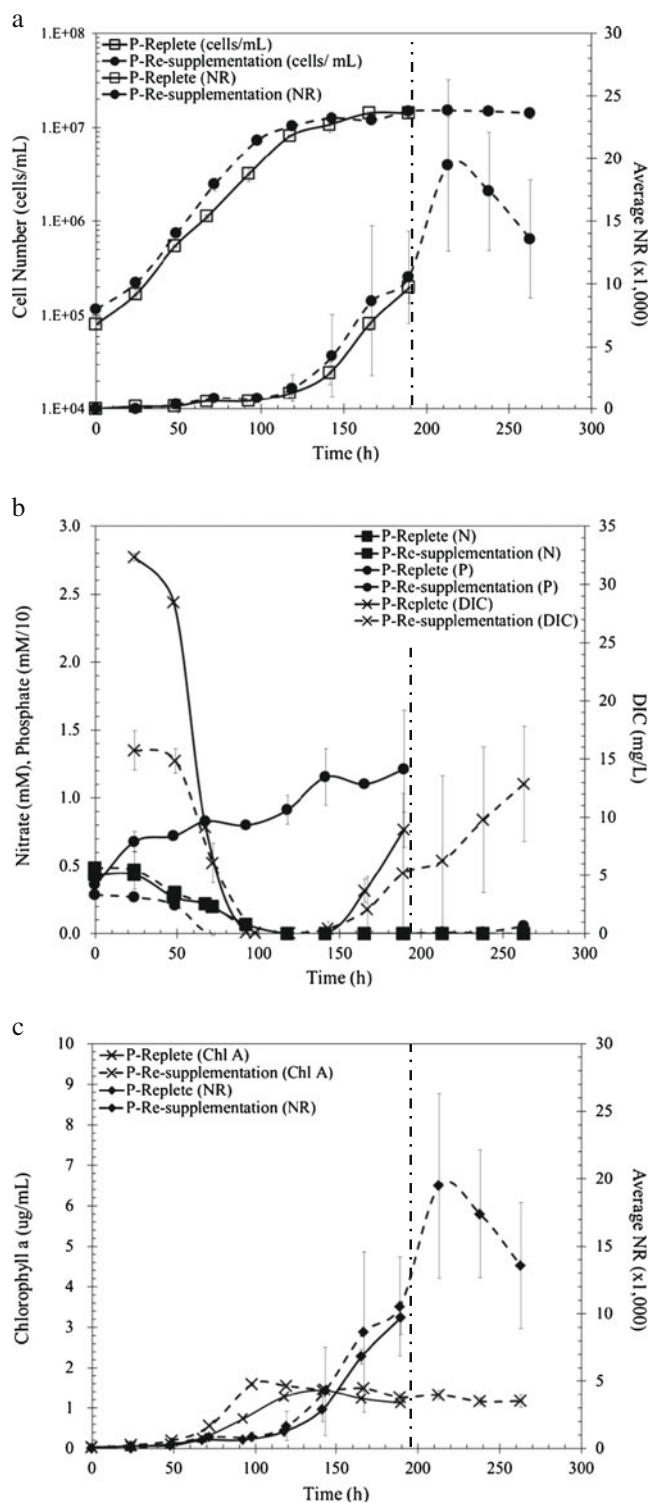


Fig. 3 *P. tricornutum* growth parameters during continued P replete conditions (solid lines) and P resupplemented (dashed lines), meaning nitrogen stress conditions. The dashed vertical line indicates where N was resupplemented at 189 h. **a** Growth curve cells per milliliters (unfilled square, filled circle) and Nile Red fluorescence intensity (unfilled square, filled circle). **b** DIC (cross), NO_3^- (filled square), PO_4^{3-} (filled circle) throughout growth (phosphate was multiplied by a scaling factor of 10). **c** Chlorophyll *a* (cross) concentrations and Nile Red fluorescence intensity (filled diamond)

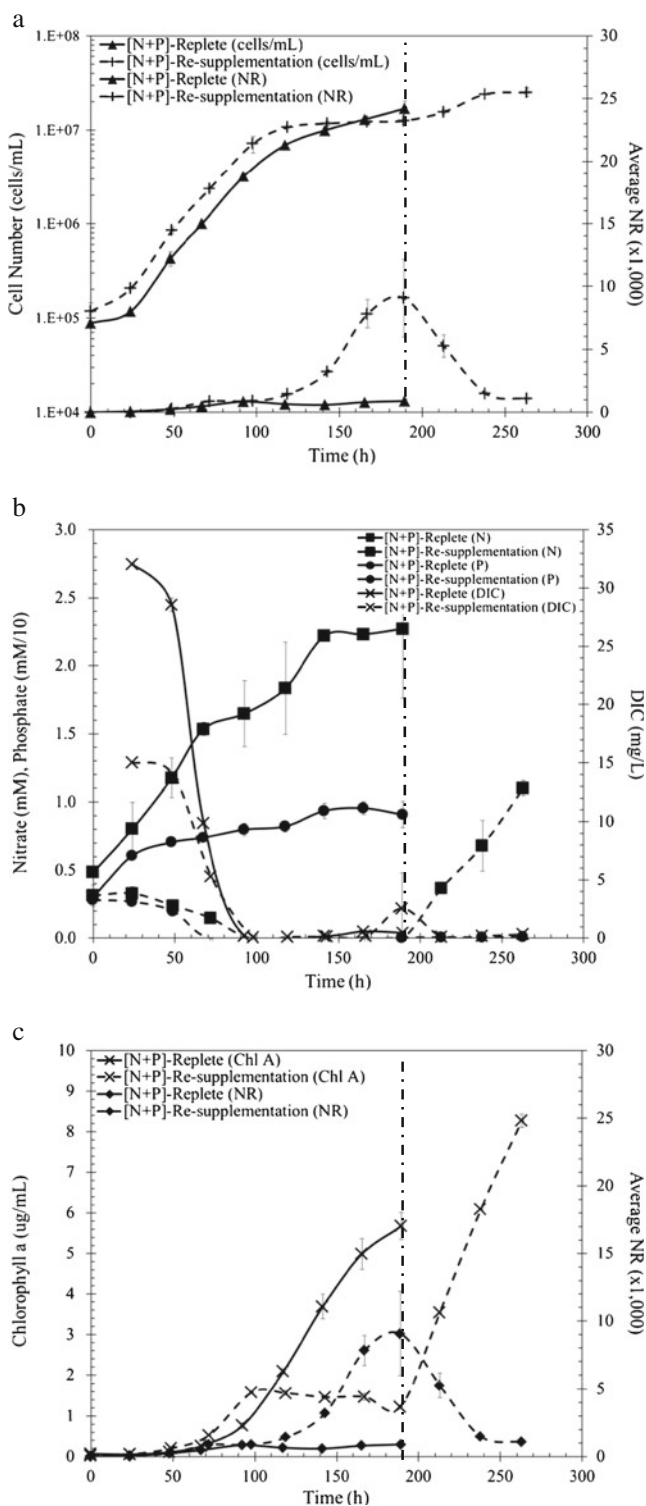


Fig. 4 *P. tricornutum* growth parameters during continued N+P replete conditions (solid lines) and N+P resupplemented (dashed lines), meaning no nutrient stress conditions. The dashed vertical line indicates where N was resupplemented at 189 h. **a** Growth curve cells per milliliter (filled triangle, plus) and Nile Red fluorescence intensity (filled triangle, plus) vs Time (h). **b** DIC (cross), NO_3^- (filled square), PO_4^{3-} (filled circle) throughout growth; phosphate was multiplied by a scaling factor of 10. **c** Chlorophyll a (cross) concentrations and Nile Red fluorescence intensity (filled diamond) vs Time (h)

Similar to resupplementation with nitrate alone, chlorophyll increased upon resupplementation with both N and P (Fig. 4c). These results indicate a significant metabolic shift from a lipid accumulation mode to cellular growth.

FAME analysis

The largest differences in NR fluorescence intensities were observed between control cells under N and P depletion and the N+P-supplemented cells. The NR fluorescence of the control culture paralleled N+P-resupplemented cells (at 119 and 189 h), before differentiating at 263 h, and these samples were selected for FAME analysis and quantification. Total FAMES were quantified based on standard curves and calculated in moles of original fatty acids per cell. The fatty acid levels for control (N+P depleted) and N+P-supplemented cells were not significantly different at the 119- and 189-h time points (Fig. 5a). However, the nutrient-depleted cells had approximately 16-fold greater FAME levels compared to nutrient-resupplemented cells (263 h). These results were supported by the NR-stained epifluorescence microscopy images (Fig. 5b and c). Cells under N+P-deplete conditions have large visible lipid bodies that fluoresce yellow, while N+P-resupplemented

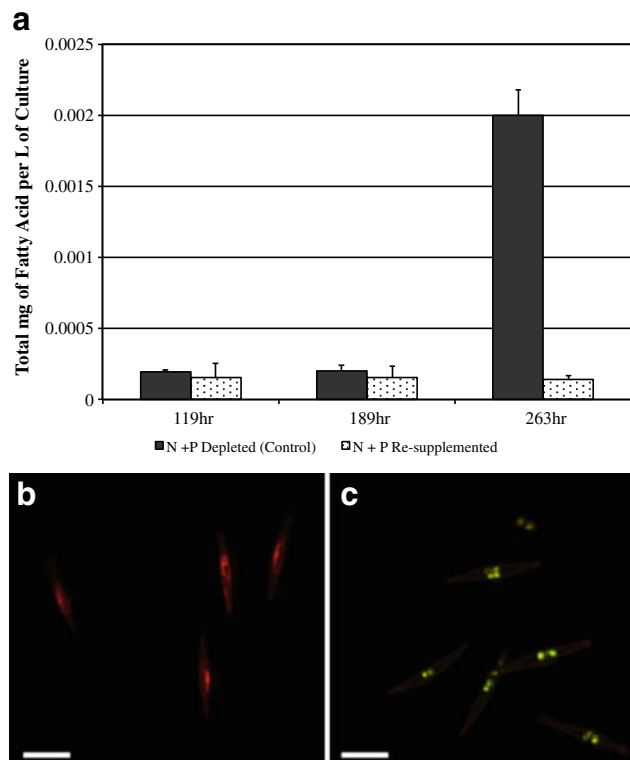


Fig. 5 *P. tricornutum* lipid accumulation. **a** Total moles of FAMES per liter of culture in control (N+P-depleted cells) compared to (N+P-resupplemented cells). **b** Cells stained with Nile Red during N+P-resupplemented conditions. **c** Cells stained with Nile Red under N+P-depleted conditions, showing lipid bodies in yellow. Scale bars, 10 μm

conditions do not have visible lipid bodies (Fig. 5b and c). The FAME profile of the control culture for *P. tricornutum* is shown in Fig. 6 on a logarithmic scale. The control profile indicates changes in fatty acid content during lipid accumulation. The most abundant three-fatty acids were hexadec-9-enoic acid, hexadecanoic acid, and 5,8,11,14,17-eicosapentaenoic acid. Hexadec-9-enoic acid and hexadecanoic acid are both C16 molecules, while 5,8,11,14,17-eicosapentaenoic acid is an unsaturated C20 compound.

Discussion

P. tricornutum has been shown to increase TAG accumulation when nutrient stressed, particularly from nitrogen and phosphorus (Burrows et al. 2012; Larson and Rees 1996; Reitan et al. 1994; Valenzuela et al. 2012; Yu et al. 2009). The goal of the described work was to investigate cellular responses when N and P were resupplemented in batch-mode postlipid accumulation. In the control condition, extracellular phosphate was depleted before nitrate but did not cause cell growth cessation. However, lipid accumulation was initiated to a small extent. This may be due to the ability of *P. tricornutum* to store phosphate internally as polyphosphate (Leitao et al. 1995). Thus, cells were most likely not completely limited because internal phosphate stores might have been available, but as exogenous nitrate depleted and the degradation of chlorophyll and recycling of amino acids proceeded (Lee et al. 2012), lipid accumulation ensued.

During exponential growth, DIC was limited due to high cell growth demand, but DIC concentration in the medium rebounded as growth stopped and lipids were accumulated. The results suggested a clear distinction of lowered carbon fixation needs during lipid accumulation compared to

cellular growth/replication. Protein production would be limited without available nitrogen; however, carbon fixation still occurs and can be directed into energy storage molecules (i.e., lipids). This represents a shift in metabolism from cellular growth to lipid accumulation in which the demand for DIC apparently decreases because cells require more carbon for biomass production than for lipid accumulation.

It has been shown that in nitrate-deprived *P. tricornutum* cells, lipid biosynthesis was predominantly de novo (Burrows et al. 2012). *P. tricornutum* can shift carbon-concentrating mechanisms (CCMs) based on DIC demand and use a C4-CCM when DIC concentration is low during photosynthetic growth at high cell densities (Valenzuela et al. 2012). Gene expression levels for TCA enzymes are largely maintained during nitrogen depletion to potentially provide precursors for nitrogen assimilation in the event more nitrogen is encountered (Hockin et al. 2012; Valenzuela et al. 2012). This explains the rapid reversal of lipid accumulation when nitrate is resupplemented to the depleted cells. Metabolism is primed for assimilation of nitrogen and can quickly shift back toward growth conditions. As soon as nitrogen becomes available, carbon can be redirected from fatty acid storage to biomass growth and existing lipids are consumed.

In the presence of sufficient nitrogen, phosphate depletion (Fig. 2) can initiate lipid accumulation but to a limited extent when compared to nitrogen (Fig. 3). The difference in cellular responses to N and P levels may be explained in the context of the Redfield ratio of 16:1 (Redfield 1934; Zhang and Hu 2011). The Redfield ratio is an empirically developed stoichiometric ratio of carbon, nitrogen, and phosphorus based upon marine phytoplankton (Redfield 1934). The physiological response to phosphate limitation (i.e., limited lipid accumulation) is different than nitrogen limitation due to the different requirements and routes for resource allocation (e.g., protein versus nucleotides). Both result in cell cycle cessation, but the relative lipid accumulation response is different. This difference is observed as a fivefold greater increase in specific fluorescence when cells were depleted of nitrate (6.9 NR-specific fluorescence) compared to cells depleted of phosphate (1.4 NR-specific fluorescence). However, when both N and P are depleted, the effects combine for the greatest increase in lipid accumulation (approximately NR-specific fluorescence) (Fig. S1a).

When cells had initiated lipid accumulation based on nutrient depletion, the resupplementation with nitrate had more of an effect on shifting cells back to a growth state via cellular increases. The shift is evident in the approximately 13-fold decrease in NR-specific signal (Fig. S1b), an increase in DIC demand, and an increase in cell abundance when nitrate was resupplemented (Fig. 2). The decrease in lipid content could be a result of direct utilization when cells are transitioning back to cell growth and/or partitioning between cells during mitosis. While the respective effects

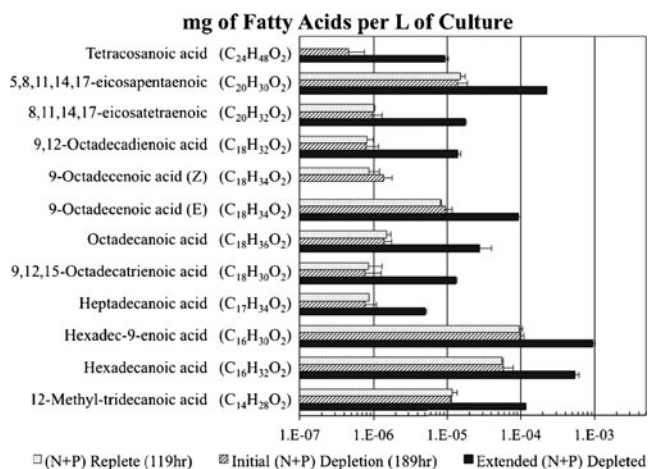


Fig. 6 *P. tricornutum* fatty acid profiles and abundance (mg/liter of culture) from control cells during hours 119, 189, and 263 of growth. Nutrient depletion occurred at hour 189. Results are shown on a logarithmic scale

are not known, when N was resupplemented, the cell number increased 1.3-fold, while the NR fluorescence number declined approximately 10-fold. In addition, lipid droplets were not observed in resupplemented cells. This result indicates that utilization played a large role in the observed lipid decrease.

However, when cells were resupplemented with phosphate, the shift away from lipid accumulation was not as drastic. Namely, lipid content did not increase, but only slightly decreased, postphosphate resupplementation. DIC consumption did not increase as observed in a high DIC demand state during exponential growth, and cell numbers did not increase. Similar results were observed by Liang et al. in 2012 in a species of *Chlorella* (Liang et al. 2012) as well as by Feng et al. in *Chlorella zofingiensis* (Feng et al. 2012). Thus, as it pertains to lipid accumulation, nitrate depletion has a greater effect than phosphate depletion in regards to *P. tricornutum*, both in terms of lipid accumulation and subsequent lipid consumption after resupplementation. One reason for this may be the difference in reducing equivalents required to utilize nitrate and phosphate. Unlike phosphate, nitrate needs to be reduced for utilization. Thus, the reduction of nitrate consumes electrons that would otherwise go towards carboxylation in the Calvin cycle or possibly fatty acid synthesis (Beardall et al. 2009; Oroszi et al. 2011). In addition, as mentioned above, nitrogen demand exerts a greater effect on resource allocation due to the ratio of C:N:P in biomass ($C_{106}:N_{16}:P_1$), and therefore, carbon and nitrogen metabolism is inherently linked via metabolites (e.g., α -ketoglutarate–glutamine–glutamate) and is enriched in biomass.

Independently, nitrate and phosphate depletion can cause lipid accumulation, but maintaining replete conditions or resupplementation of media can drastically inhibit or reduce lipid accumulation, respectively (Fig. 4). In *P. tricornutum*, nitrogen and phosphorus depletion together have a greater impact on lipid accumulation than compared to the nutrient effects independently. The metabolic mechanisms between phosphate and nitrate stress are different, but the metabolic consequences could be similar. Cyclins (*cycs*) and cyclin-dependent kinases (CDKs) work together to ensure correct passage through the cell cycle. Many different cyclins and CDKs have been shown to sense and respond to nutrient availability (Huysman et al. 2010), such as phosphate and nitrate. Our recent results showed that similar cyclins responded to nutrient stress as detected via transcriptome profiling in *P. tricornutum* (Valenzuela et al. 2012). Thus, there is a molecular consequence to nutrient deprivation leading to cellular responses that favor lipid accumulation, such as the increase in acetyl-CoA carboxylase during initial lipid accumulation (Valenzuela et al. 2012). However, the ability to accumulate lipids can be quickly reversed in response to nutrients and might suggest the presence of signal transduction systems to coordinate cellular growth

versus lipid accumulation in a nutrient-dependent manner. Therefore, the manipulation of nutrient-dependent cyclins could be used to control resource allocation via cell cycle inhibition.

FAME analysis quantifies how specific nutrient depletion is critical for lipid accumulation in *P. tricornutum* (Figs. 5 and 6). The three major fatty acids that increased were hexadec-9-enoic acid, hexadecanoic acid, and 5,8,11,14,17-eicosapentaenoic acid. Our results coincide with results from a recent study by Řenzanka et al. (2012), where these three fatty acids were also observed most prevalent in *P. tricornutum*. The authors reported an 85 % increase in TAG assemblies with 5,8,11,14,17-eicosapentaenoic acid and two palmitic fatty acids (hexadec-9-enoate and hexadecanoic acid) based on phosphate starvation. Our results are similar and the slight differences could be attributed to additional nitrogen depletion stress. In both studies, an increase in C16 and C16:1 fatty acids was observed in response to nutrient deprivation, and total lipids increased 16-fold with depletion of nitrate and phosphate compared to resupplementation conditions (Fig. 5).

In conclusion, *P. tricornutum* accumulated lipid under phosphate depletion and under nitrate depletion independently, but the accumulation was magnified when both nutrients were depleted in batch mode. Under N+P-replete conditions, the diatom does not accumulate lipid because carbon may be directed into cellular biomass production and growth as evident by higher cell numbers, high DIC demand, and low to no lipid accumulation. Resupplementation with phosphate after lipid accumulation can decrease accumulation and increase consumption of fatty acid stores as cells shift away from a lipid-accumulating state. Nitrate resupplementation shuts down lipid accumulation and presumably increases lipid consumption to a greater extent than phosphate resupplementation, as cells shift to a cellular growth state signified by increased cell numbers. The resupplementation with both nitrate and phosphate arrested lipid accumulation and shifted cells to growth conditions with a corresponding consumption of lipids. Cell numbers and DIC demand increased, signifying a metabolic shift back to biomass growth away from lipid accumulation. FAME profiles remained similar throughout nutrient-deplete growth with the largest increases in the C16 fatty acids (hexadec-9-enoic acid and hexadecanoic acid). An understanding of cellular responses to carbon, nitrogen, and phosphorus ratios in the context of cellular growth and lipid accumulation is essential for improved control and biomass quality. In addition, different mixed nutrient sources (e.g., wastewater) will have different ratios of N and P, and will impact microalga physiology as well as the accompanying microbial community in different ways. Thus, when growing algae for the purpose of biofuel production, the control of exogenous nutrient levels is imperative to control cellular growth versus lipid accumulation

regardless of whether algae are being cultivated in raceway ponds, photobioreactors, or wastewater effluents.

Acknowledgments The authors would like to thank all members of the MSU Algal Biofuels Group for helpful discussions. Support was provided by the Air Force Office of Scientific Research (DOD-AFOSR grant FA9550-09-1-0243), the Molecular Bioscience Program at Montana State University, and NSF-EPSCoR. We are also thankful for laboratory contributions by Erika Whitney. We would also like to thank the Murdock Charitable Trust and NIH Cobre 5P20RR02437-03 for support of the mass spectrometry facility at MSU. This material is also based upon work supported by the National Science Foundation under CHE-1230632.

Open Access This article is distributed under the terms of the Creative Commons Attribution License which permits any use, distribution, and reproduction in any medium, provided the original author(s) and the source are credited.

References

- Aslan S, Kapdan IK (2006) Batch kinetics of nitrogen and phosphorus removal from synthetic wastewater by algae. *Ecol Eng* 28:64–70
- Beardall J, Ihnken S, Quigg A (2009) Gross and net primary production: closing the gap between concepts and measurements. *Aquat Microbial Ecol* 56:113–122
- Bowler C, Allen AE, Badger JH, Grimwood J, Jabbari K, Kuo A, Maheswari U, Martens C, Maumus F et al (2008) The *Phaeodactylum* genome reveals the evolutionary history of diatom genomes. *Nature* 456:239–244
- Brown LR (2006) Plan B 2.0: rescuing a planet under stress and a civilization in trouble. Updated and Expanded. W. W. Norton, New York, NY
- Burrows EH, Bennette NB, Carrieri D, Dixon JL, Brinker A, Frada M, Baldassano SN, Falkowski PG, Dismukes GC (2012) Dynamics of lipid biosynthesis and redistribution in the marine diatom *Phaeodactylum tricoratum* under nitrate deprivation. *Bioenerg Res* 5:876–885
- Chisti Y (2007) Biodiesel from microalgae. *Biotechnol Adv* 25:294–306, Elsevier
- Cooksey KE, Cooksey B (1974) Calcium deficiency can induce the transition from oval to fusiform cells in cultures of *Phaeodactylum tricoratum* Bohlin. *J Phycol* 10:89–90
- Cooksey KE, Guckert JB, Williams SA, Callis PR (1987) Fluorometric determination of the neutral lipid content of microalgal cells using Nile Red. *J Microbiol Meth* 6:333–345
- Courchesne NMD, Parisien A, Wang B, Lan CQ (2009) Enhancement of lipid production using biochemical, genetic and transcription factor engineering approaches. *J Biotechnol* 141:31–41
- Dukes JS (2003) Burning buried sunshine: human consumption of ancient solar energy. *Clim Chang* 61:31–44
- Falkowski PG, Raven JA (1997) Aquatic photosynthesis. Blackwell, Oxford
- Feng P, Deng Z, Fan L, Hu Z (2012) Lipid accumulation and growth characteristics of *Chlorella zofingiensis* under different nitrate and phosphate concentrations. *J Biosci Bioeng* 114:405–410
- Field CB (1998) Primary production of the biosphere: integrating terrestrial and oceanic components. *Science* 281:237–240
- Gardner R, Peters P, Peyton B, Cooksey KE (2010) Medium pH and nitrate concentration effects on accumulation of triacylglycerol in two members of the chlorophyta. *J Appl Phycol* 23:1005–1016
- Granum E, Raven JA, Leegood RC (2005) How do marine diatoms fix 10 billion tonnes of inorganic carbon per year? *Can J Bot* 83:898–908
- Greenwell HC, Laurens LML, Shields RJ, Lovitt RW, Flynn KJ (2010) Placing microalgae on the biofuels priority list: a review of the technological challenges. *J Roy Soc Interface* 7:703–726
- Hildebrand M (2008) Diatoms, biomineralization processes, and genomics. *Chem Rev* 108:4855–4874
- Hockin NL, Mock T, Mulholland F, Kopriva S, Malin G (2012) The response of diatom central carbon metabolism to nitrogen starvation is different from that of green algae and higher plants. *Plant Physiol* 158:299–312
- Hoffmann JP (2002) Wastewater treatment with suspended and nonsuspended algae. *J Phycol* 34:757–763
- Hu Q, Sommerfeld M, Jarvis E, Ghirardi M, Posewitz M, Seibert M, Darzins A (2008) Microalgal triacylglycerols as feedstocks for biofuel production: perspectives and advances. *Plant J* 54:621–639
- Huysman MJ, Martens C, Vandepoele K, Gilard J, Rayko E, Heijde M, Bowler C, Inzé D, Van de Peer Y et al (2010) Genome-wide analysis of the diatom cell cycle unveils a novel type of cyclins involved in environmental signaling. *Genome Biol* 11:R17
- Larson TR, Rees TAV (1996) Changes in cell composition and lipid metabolism mediated by sodium and nitrogen availability in the marine diatom *Phaeodactylum tricoratum* (Bacillariophyceae). *J Phycol* 32:388–393
- Lee DY, Park JJ, Barupal DK, Fiehn O (2012) System response of metabolic networks in *Chlamydomonas reinhardtii* to total available ammonium. *Mol. Cellular Proteomics* 11:973–988
- Leitao JM, Lorenz B, Bachinski N, Wilhelm C, Muller WEG, Schroder HC (1995) Osmotic-stress-induced synthesis and degradation of inorganic polyphosphates in alga *Phaeodactylum tricoratum*. *Mar Ecol Prog Ser* 121:279–288
- Liang K, Zhang Q, Gu M, Cong W (2012) Effect of phosphorus on lipid accumulation in freshwater microalga *Chlorella* sp. *J Appl Phycol* 25:311–318
- Mallick N (2002) Biotechnological potential of immobilized algae for wastewater N, P and metal removal: a review. *BioMetals* 15:377–390
- Martino AD, Meichenin A, Shi J, Pan K, Bowler C (2007) Genetic and phenotypic characterization of *Phaeodactylum tricoratum* (Bacillariophyceae) accessions. *J Phycol* 43:992–1009
- Mus F, Toussaint JP, Cooksey KE, Gerlach R, Fields MW, Peyton BM, Carlson RP (2013) Physiological and molecular analysis of carbon source supplementation and pH stress induced lipid accumulation in marine diatom *Phaeodactylum tricoratum*. *Appl Microbiol Biotechnol* 97:3625–3642
- Oroszi S, Jakob T, Wilhelm C, Harms H (2011) Photosynthetic energy conversion in the diatom *Phaeodactylum tricoratum*: measuring by calorimetry, oxygen evolution and pulse-amplitude modulated fluorescence. *J Therm Anal Calorim* 104:223–231
- Oudot-Le Secq M-P, Grimwood J, Shapiro H, Armbrust EV, Bowler C, Green BR (2007) Chloroplast genomes of the diatoms *Phaeodactylum tricoratum* and *Thalassiosira pseudonana*: comparison with other plastid genomes of the red lineage. *Mol Genet Genomics* 277:427–439
- Pittman JK, Dean AP, Osundeko O (2011) The potential of sustainable algal biofuel production using wastewater resources. *Bioresource Technol* 102:17–25
- Porra R (2002) The chequered history of the development and use of simultaneous equations for the accurate determination of chlorophylls a and b. *Photosynth Res* 73:149–156
- Provasoli L, McLaughlin JJA, Droop MR (1957) The development of artificial media for marine algae. *Archiv Mikrobiologie* 25:392–428
- Redfield A (1934) On the proportions of organic derivatives in sea water and their relation to the composition of plankton. *James Johnstone Memorial* 1934:176–192

- Reitan KI, Rainuzzo JR, Olsen Y (1994) Effect of nutrient limitation on fatty acid and lipid content of marine microalgae. *J Phycol* 30:972–979
- Řezanka T, Lukavský J, Nedbalová L, Kolouchová I, Sigler K (2012) Effect of starvation on the distribution of positional isomers and enantiomers of triacylglycerol in the diatom *Phaeodactylum tricorutum*. *Phytochemistry* 80:17–27
- Round FE, Crawford RM, Mann DG (1990) *The diatoms: biology and morphology of the genera*. Cambridge University Press, London
- Sheehan, J. (1998). A look back at the US Department of Energy's aquatic species program: biodiesel from algae, <http://www.nrel.gov/biomass/pdfs/24190.pdf>.
- Valenzuela J, Mazurie A, Carlson RP, Gerlach R, Cooksey KE, Peyton BM, Fields MW (2012) Potential role of multiple carbon fixation pathways during lipid accumulation in *Phaeodactylum tricorutum*. *Biotechnol Biofuels* 5:40
- Yu ET, Zendejas FJ, Lane PD, Gaucher S, Simmons BA, Lane TW (2009) Triacylglycerol accumulation and profiling in the model diatoms *Thalassiosira pseudonana* and *Phaeodactylum tricorutum* (Baccilariophyceae) during starvation. *J Appl Phycol* 21:669–681
- Zhang Q, Hu G (2011) Effect of nitrogen to phosphorus ratios on cell proliferation in marine micro algae. *Chin J Ocean Limnol* 29:739–745